Biochemical and Biophysical Research Communications 439 (2013) 109–114

Contents lists available at ScienceDirect

Biochemical and Biophysical Research Communications

journal homepage: www.elsevier.com/locate/ybbrc

The crystal structure of D-mandelate dehydrogenase reveals its distinct substrate and coenzyme recognition mechanisms from those of 2-ketopantoate reductase

Akimasa Miyanaga *, Shinsuke Fujisawa, Nayuta Furukawa, Kazuhito Arai, Masahiro Nakajima, Hayao Taguchi

Department of Applied Biological Science, Faculty of Science and Technology, Tokyo University of Science, 2641 Yamazaki, Noda, Chiba 278-8510, Japan

ARTICLE INFO

Article history:
Received 1 August 2013
Available online 13 August 2013

Keywords:
D-Mandelate dehydrogenase
2-Ketopantoate reductase
Coenzyme specificity
Substrate specificity
Crystal structure

ABSTRACT

D-Mandelate dehydrogenases (D-ManDHs), belonging to a new D-2-hydroxyacid dehydrogenase family, catalyze the conversion between benzoylformate and D-mandelate using NAD as a coenzyme. We determined the first D-ManDH structure, that of ManDH2 from *Enterococcus faecalis* IAM10071. The overall structure showed ManDH2 has a similar fold to 2-ketopantoate reductase (KPR), which catalyzes the conversion of 2-ketopantoate to D-pantoate using NADP as a coenzyme. They share conserved catalytic residues, indicating ManDH2 has the same reaction mechanism as KPR. However, ManDH2 exhibits significant structural variations in the coenzyme and substrate binding sites compared to KPR. These structural observations could explain their different coenzyme and substrate specificities.

1. Introduction

D-2-Hydroxyacid dehydrogenases (D-2-HydDHs) catalyze the oxidation–reduction between 2-ketoacids and D-2-hydroxyacids using NAD or NADP as a coenzyme. Various D-2-HydDHs such as D-phosphoglycerate [1], D-lactate [2–4], D-hydroxyisocaproate [5], and D-glycerate[6] dehydrogenases share a common protein structure, and constitute a large D-2-HydDH family [7], together with other dehydrogenases such as formate [8] and L-alanine [9] dehydrogenases. The substrate recognition by these enzymes has been well studied, and subtle structural changes such as amino acid substitutions were reported to cause drastic changes in substrate specificity [10–14]. As for coenzyme specificity, although most D-2-HydDH enzymes exhibit strict specificity toward NAD, amino acid substitutions were reported to result in alteration of coenzyme specificity [14–16]. Thus, D-2-HydDH family enzymes exhibit wide and variable catalytic properties. However, no enzymes belonging to the D-2-HydDH family have been reported to exhibit high catalytic activity toward C3-branched substrates.

We previously reported the cloning and characterization of a D-mandelate dehydrogenase (D-ManDH), ManDH2, catalyzing the conversion between benzoylformate and D-mandelate from *Enterococcus faecalis* IAM10071 (Fig. 1A) [17,18]. Surprisingly, the sequences of ManDH2 show no homology with those of known D-2-HydDHs. Sequence analysisrevealed ManDH2 shows weak sequence similarity to 2-ketopantoate reductases (KPRs) (Fig. 2), which catalyze the conversion of 2-ketopantoate to D-pantoate (Fig. 1B) [19]. This indicates D-ManDHs constitute a new family of D-2-hydroxyacid dehydrogenases acting on C3-branched substrates together with KPRs. However, D-ManDHs and KPRs do not share substrate specificity. KPRs prefer hydrophilic substrates including 2-ketopantoate, while D-ManDHs prefer bulkier hydrophobic substrates such as 2-ketoisovalerate, benzoylformate and 2-ketoisocaproate. In addition, D-ManDHs show strict coenzyme specificity for NAD, but KPRsuse NADP as a coenzyme. Based on the results of detail functional and structural analysis of *Escherichia coli* KPR (EcKPR), substrate and coenzyme recognition mechanisms have been proposed for KPRs [19–21]. However, how D-ManDHs acquire the distinct substrate and coenzyme specificities has remained unclear because D-ManDHs have been less characterized so far. Here we report the crystal structure of ManDH2. The ManDH2 structure shows that there are significant structural variations in the coenzyme and substrate binding sites between

Abbreviations: CENDH, *N*-(1-D-carboxyethyl)-L-norvaline dehydrogenase from *Arthrobacter* sp.; D-2-HydDH, D-2-hydroxyacid dehydrogenase; EcKPR, 2-ketopantoate reductase from *Escherichia coli*; KPR, 2-ketopantoate reductase; D-ManDH, D-mandelate dehydrogenase; ManDH2, D-mandelate dehydrogenase from *Enterococcus faecalis* IAM10071; rmsd, root mean square deviation..

* Corresponding author. Present address: Department of Chemistry, Graduate School of Science and Engineering, Tokyo Institute of Technology, 2-12-1 O-okayama, Meguro-ku, Tokyo 152-8551, Japan. Fax: +81 3 5734 2607.
E-mail address: miyanaga.a.aa@m.titech.ac.jp (A. Miyanaga).

0006-291X/$ - see front matter © 2013 Elsevier Inc. All rights reserved.
http://dx.doi.org/10.1016/j.bbrc.2013.08.019

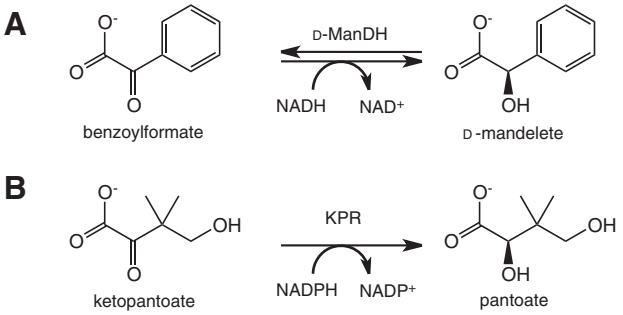

Fig. 1. Reaction schemes for D-ManDHs (A) and KPRs (B).

ManDH2 and EcKPR. Thus our work provides an insight into the substrate and coenzyme recognition mechanisms of the new family of D-2-hydroxyacid dehydrogenases acting on C3-branched substrates.

2. Materials and methods

2.1. Preparation of purified recombinant ManDH2

E. coli BL21-Gold (DE3) pLysS cells (Takara, Ohtsu, Japan) harboring pET3a-*manDH2* plasmid [18] were grown at 37 °C in 2 × YT medium (1.6% tryptone, 1.0% yeast extract and 0.5% NaCl) containing 150 μg/ml ampicillin. After OD_{600} reached 0.5, protein expression was induced by addition of 1 mM IPTG. The cells were then cultured for an additional 4 h at 27 °C. From cell-free extracts prepared by sonication, the recombinant ManDH2 protein was purified by ammonium sulfate precipitation, and Butyl-Toyopearl (Tosoh, Tokyo, Japan) and UnoQ (Biorad, Hercules, CA, USA) column chromatographies. The enzyme assay was performed as described previously [18].

2.2. Crystallization of ManDH2

ManDH2 apo crystals were grown from a 1:1 mixture of a protein solution (10 mg/ml in 10 mM Tris–HCl (pH 7.5)) and a reservoir solution (0.085 M HEPES-Na (pH 7.5), 0.17 M ammonium acetate and 22.5% PEG8000) using the hanging-drop vapor diffusion method at 25 °C. ManDH2 cocrystals with NADH were grown from a 1:1 mixture of a protein solution (10 mg/ml in 10 mM Tris–HCl (pH 7.5) and 10 mM NADH) and a reservoir solution (0.1 M Tris–HCl (pH 7.0), 0.2 M calcium acetate, and 20%PEG3350) using the hanging-drop vapor diffusion method at 25 °C. Prior to X-ray data collection, crystals were transferred in the reservoir solution containing 25% (v/v) glycerol as a cryoprotectant and flash-frozen in the liquid nitrogen stream. X-ray data were collected using beamline AR-NW12A (Photon Factory, Tsukuba, Japan). All diffraction data were indexed, integrated and scaled using the program iMosflm [22]. The initial phases were determined by the molecular replacement method using the program Molrep [23]. The crystal structure of *E. faecalis* putative 2-dehydropantoate reductase (PDB code: 2EW2) was used as a search model. The program ARP/wARP [24] was used for automatic initial protein modelbuilding. Coot [25] was used for visual inspection and manual rebuilding of the model. Refmac [26] was used for refinement. The figures were prepared using PyMOL [27]. The coordinates and structure factors have been deposited in the Protein Data Bank (PDB codes: 3WFI and 3WFJ).

2.3. Site-directed mutagenesis

An expression plasmid, pET3a-*manDH2* [18], was used for site-directed mutagenesis. Site-directed mutagenesis was performed with a QuikChange site-directed mutagenesis kit (Stratagene, La Jolla, CA, USA) using the following oligonucleotides. Oligonucleotide 5′-CACTATTCTATTTATCGCGCAGCATGTGTGAACGGAACAATG-3′ and its complementary oligonucleotide were used to obtain K187A mutant. The mutation was confirmed by determining the nucleotide sequence. This plasmid was transformed into *E. coli*

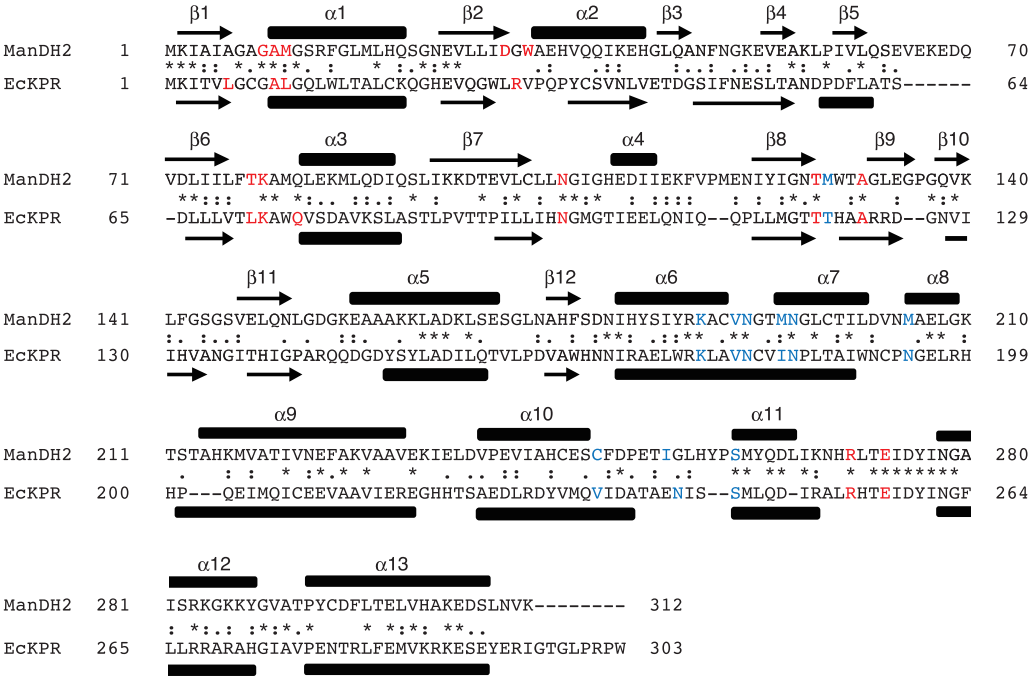

Fig. 2. Amino acid sequence alignment of ManDH2 and EcKPR performed with ClustalW. Residues involved in the coenzyme binding are shown in red. Residues proposed for the substrate-binding are shown in blue. The secondary structural elements of ManDH2 and EcKPR are indicated by bars above or below the sequence. (For interpretation of the references to color in this figure legend, the reader is referred to the web version of this article.)

BL21-Gold (DE3) pLysS cells, and the mutant enzyme was expressed, purified, and assayed as described above.

3. Results and discussion

3.1. Overall structure of ManDH2

We have determined the crystal structure of apo ManDH2 at 2.0 Å resolution (Table 1). In the apo ManDH2 structure, there are two ManDH2 molecules per crystallographic asymmetric unit. The result of gel-filtration chromatography showed that the ManDH2 protein actually exists as a homodimer in solution (data not shown). The enzyme contains N-terminal (residues 1–176) and C-terminal domains (residues 180–311) connected by a hinge region (residues 177–179) (Fig. 3A). The N-terminal domain shows a typical Rossmann-type α/β fold. It has a central 8-stranded β-sheet (β1, β2, β5–8, β11 and β12) flanked by 5 α-helices and an additional 4-stranded β-sheet (β3, β4, β9 and β10). In contrast, the C-terminal domain has 8 α-helices that form an α-helical fold. The C-terminal domain interacts with the C-terminal domain of the complementary subunit through a relatively small contact area (1048 Å^2) to form a homodimer.

A search for structurally related proteins using the program Dali [28] indicated structural homology to NADPH-dependent EcKPR [19–21], which has been well characterized (Z score = 29.6, root mean square deviation [rmsd] of 3.2 Å, and sequence identity of 25%), as expected from amino acid sequence comparison. EcKPR is monomeric, different from dimeric ManDH2. Dali analysis also showed structural similarity to *N*-(1-D-carboxyethyl)-L-norvaline dehydrogenase (CENDH) [29] of *Arthrobacter* sp. (Z score = 22.2, rmsd of 3.5 Å, and sequence identity of 18%), which is the most similar NADH-dependent dehydrogenase. CENDH was also reported to be a homodimer, which shows a similar dimeric interface and dimeric conformation to ManDH2.

Comparison of secondary structural elements revealed the N-terminal region (Asp30–Val71) of ManDH2 shows significant structural deviation from that of EcKPR (Figs. 2 and 3B). The insertion of an additional helix α2 comprising Ala33–His42 leads to 2.5 Å movement of the β-sheet pairs of β3, β4, β9 and β10 away from the domain–domain interface. The organization of secondary structural elements in the N-terminal domain of ManDH2 rather resembles that of CENDH (Supplementary Fig. 1). An additional helix α2 is also observed in CENDH. In contrast, the C-terminal domain of ManDH2 shares similar structural features with that of EcKPR.

Table 1
Data collection and refinement statistics.

Datasets	ManDH2 apo	ManDH2 NADH
Data collection statistics		
Beamline	PF-AR NW12A	PF-AR NW12A
Wavelength (Å)	1.00	1.00
Space group	$P2_1$	$P2_1$
Unit-cell parameters		
a (Å)	84.80	115.65
b (Å)	40.68	103.44
c (Å)	88.94	119.74
β (°)	105.47	90.01
Resolution (Å)	37.9–2.00	20.0–2.80
(Outer shell)	(2.11–2.00)	(2.87–2.80)
Unique reflections	37,418 (4,909)	68,132 (4,560)
Completeness (%)	93.1 (84.9)	98.0 (98.0)
R_{merge} (%)	4.8 (16.4)	8.0 (26.1)
$I/\sigma(I)$	16.1 (6.0)	11.1 (4.8)
Refinement statistics		
R_{fac} (%)	18.5	23.9
R_{free} (%)	22.4	30.6
No. of waters	322	279

3.2. Complex structure of ManDH2 with NADH coenzyme

In order to clarify the structural basis of the coenzyme specificity, we also determined the complex structure of ManDH2 with NADH at 2.8 Å resolution (Table 1). In this complex structure, there are eight ManDH2 molecules per crystallographic asymmetric unit. Each eight ManDH2 monomer shares a closed conformation in asymmetric unit. The NADH binding likely causes the C-terminal domain to rotate 18° around the hinge axis toward the N-terminal domain (Fig. 3C). This coenzyme induced domain closure was observed in several dehydrogenases [21,30–33]. For example, EcKPR was reported to show hinge bending domain closure induced by the binding of coenzyme and substrate, based on comparison of the ternaryEcKPR-NADP$^+$-pantoate complex structure with the apo EcKPR structure [21]. However, other dehydrogenases including EcKPR were reported to show relatively smaller domain rotation around the hinge axis. EcKPR, liver alcohol dehydrogenase, *Pseudomonas* sp. formate dehydrogenase and *Clostridium symbiosum* glutamate dehydrogenase exhibit about 14°, 10°, 7.5° and 14° rotation, respectively, around the hinge axis. Structural comparison revealed that apo ManDH2 adopts a more open conformation compared to other apo dehydrogenase structures. This more open apo ManDH2 structure probably causes the relatively large conformational change during coenzyme binding.

The bound NADH coenzyme is located in the cleft between the N-terminal domain and the C-terminal domain (Fig. 3C). Each part of the NADH molecule interacts with ManDH2. The adenine ring of NADH is sandwiched between the indole side-chain of Trp32 and the aliphatic side-chain of Arg270 (Fig. 4A). These two residues provide a hydrophobic pocket to anchor the adenine ring through stacking interaction. The adenosine ribose 2′ and 3′-hydroxyl groups form hydrogen bonds with the side-chain carboxyl group of Asp30. The presence of an acidic residue at the end of second strand β2 is a typical feature of NADH-dependent oxidoreductases such as CENDH [29,34]. The previous mutational studies suggested the interaction between this acidic residue and the adenosine ribose of NADH is important for the coenzyme specificities of several NADH-dependent oxidoreductases [34–38]. The pyrophosphate moiety is located adjacent tothe glycine-rich region, Gly7–Gly12 (GAGAMG). This glycine-rich region, which is located at the beginning of first helix α1 and is a common nucleotide binding site in dehydrogenases [39], forms a tight turn to allow interactions between the pyrophosphate moiety and the main-chain amide groups of Ala10 and Met11. In addition, the side-chain amine groups of Lys79 and Arg270 form salt bridges with the pyrophosphate moiety from the opposite side of the glycine-rich region. The nicotinamide-ribose hydroxyl groups form hydrogen bonds with the side-chain carboxylate group of Glu273 and the side-chain amide group of Asn105. The nicotinamide ring is recognized by Met11 and Thr127 through hydrophobic interactions. The nicotinamide carbonyl and amide groups form hydrogen bonds with the main-chain amide and carbonyl of Ala131. Thus, most residues involved in the interaction with NADH are located in the N-terminal domain, but some significant C-terminal domain residues such as Arg270 and Glu273 are also involved in NADH binding. The participation of Arg270 and Glu273 appears to facilitate the domain closure through the interaction with NADH.

The coenzyme binding site comparison between ManDH2 and EcKPR indicated that the interactions with pyrophophate and nicotinamide ribose moieties are almost identical. However, there are significant structural differences in the adenosine binding pocket between them (Fig. 4B). In EcKPR, Arg31, which is replaced by

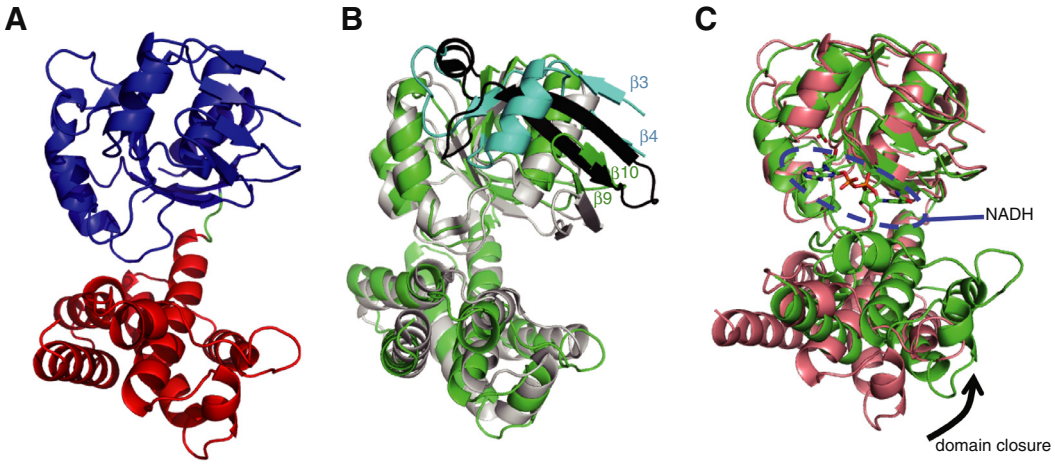

Fig. 3. Overall structure of ManDH2. (A) Ribbon drawing diagram of ManDH2. The N-terminal domain, hinge loop region and C-terminal domain are shown in blue, green and red, respectively. (B) Superimpositioning of the apo ManDH2 structure with the apo EcKPR structure. ManDH2 and EcKPR are shown in green and gray, respectively. The Asp30–Val71 region of ManDH2 and the corresponding region of EcKPR are shown in light blue and black, respectively. (C) Superimpositioning of the ManDH2 binary complex structure with the apo ManDH2 structure. The apo structure and complex structure are shown in light brown and green, respectively. The NADH molecule bound to the complex structure is shown as stick model. NADH binding site is indicated by the blue dotted line.

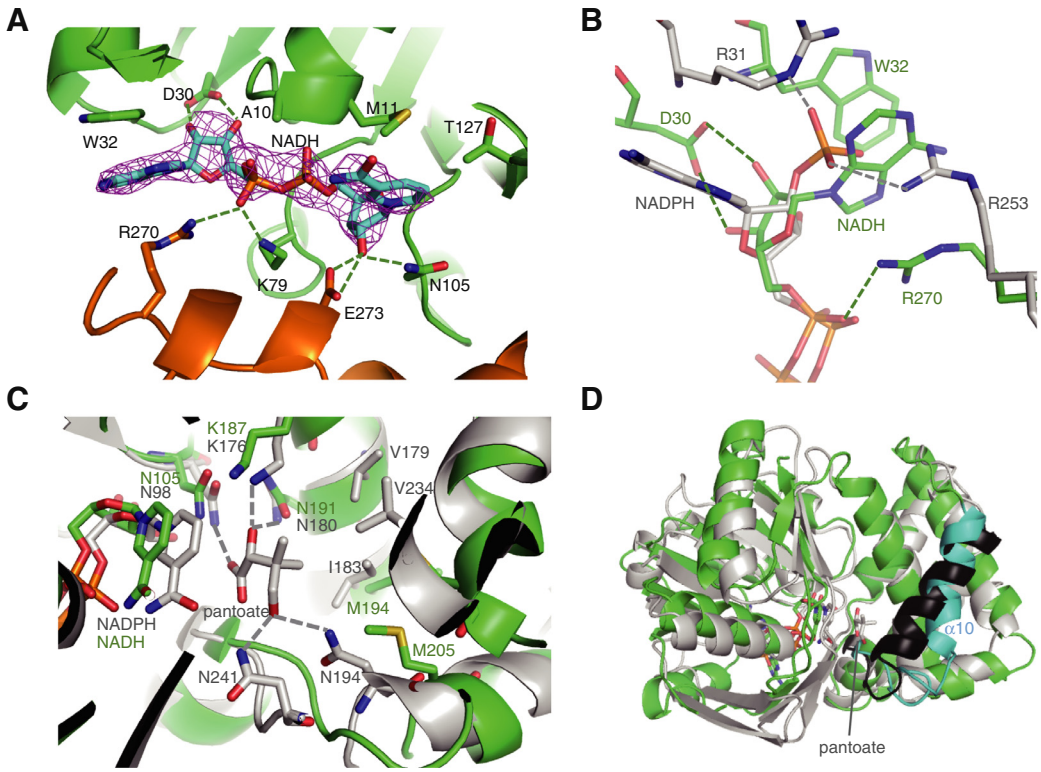

Fig. 4. The coenzyme and substrate binding sites in the ManDH2 structure. (A) Interaction between NADH and ManDH2. The ManDH2 N-terminal domain, C-terminal domain and NADH are shown in green, orange and cyan, respectively. An F_o–F_c electron density map contoured at 2.5σ was constructed prior to incorporation of an NADH molecule into the model structure. The residues shown as a stick model are important residues for NADH binding. Hydrogen bonds and salt bridge interactions are indicated by green dashed lines. (B) Superimpositioning of the ManDH2 NADH-binding site on the EcKPR NADPH-binding site. The ManDH2 and EcKPR structures are shown in green and gray, respectively. Specific interactions of the coenzyme with ManDH2 and EcKPR are indicated by green and gray dashed lines, respectively. (C) Superimpositioning of the ManDH2 substrate-binding site on the EcKPR substrate-binding site. The ManDH and EcKPR structures are shown in green and gray, respectively. Hydrogen bonds between EcKPR and pantoate are indicated by gray dashed lines. (D) Superimpositioning of the overall ManDH2 complex structure on the overall EcKPR complex structure. ManDH2 and EcKPR are shown in green and gray, respectively. The Val237–Ser260 region of ManDH2 and the corresponding region of EcKPR are shown in light blue and black, respectively.

Gly31 in ManDH2, forms a salt bridge interaction with the 2′-phosphate group of NADPH. Arg253 of EcKPR corresponding to Arg270 of ManDH2 swings by around 4 Å to form an additional salt bridge with the 2′-phosphate group. In the case of EcKPR, in addition, the adenine group is located in a hydrophobic pocket defined by Leu6, Arg31, Leu71 and Gln75. ManDH2 has a similar hydrophobic pocket at the equivalent position, but the side-chains of Gln62 and Met86 extend toward the hydrophobic pocket and appear to pre-

vent the binding of the adenine ring of NADH with their bulky side-chains. Instead, Asp30 and Trp32 of ManDH2, which are not conserved in KPRs, contribute to the architecture of the adenosine binding pocket, as described above. The Asp30–Gly31–Trp32 motif is highly conserved among putative ManDH homologous genes. This structural variation of the binding site leads to a striking conformational difference in the coenzyme. The adenosine moiety in ManDH2 is rotated by 92° around the pyrophosphate moiety so that it is accommodated in the unique binding pocket of ManDH2. The deviation of the orientation of both the adenine and ribose rings in enzymes in the same family was also reported for other NAD(P)H-dependent oxidoreductases such as the ASADH family [40]. For these enzymes, the various coenzyme preferences are attributed to differences in the coenzyme binding conformation and coenzyme binding pocket architecture.

These structural features may explain why ManDH2 strictly utilizes only NADH as a coenzyme. As described above, the Asp30 carboxylate group attracts both the 2′ and 3′-hydroxyl groups of the adenosine ribose moiety through hydrogen bonds. In addition, Trp32 stabilizes the adenine ring through an aromatic stacking interaction. Thus, ManDH2 favors a twisted conformation of the adenosine moiety of NADH through these interactions. However, NADPH is unfavorable for ManDH2 because the extra 2′-phosphate group of NADPH causes steric hindrance and electrostatic repulsion of relatively large and negatively charged Asp30.

3.3. Substrate-binding pocket of ManDH2

We also attempted to cocrystallize ManDH2 with NADH and-mandelate to determine the ternary structure, but no electron density corresponding to mandelate was observed. However, comparison with the ternary complex structure of EcKPR with $NADP^+$ and pantoate allowed us to speculate the substrate-binding mode in ManDH2. In the EcKPR-$NADP^+$-pantoate ternary structure, Lys176, which is proposed to be a general acid, is located close to the C2 oxygen of pantoate [21]. Ciulli et al. proposed the importance of Asn98 and Glu256 in addition to Lys176 in EcKPR. These residues provide the hydrogen bonding network for the correct cofactor conformation required for productive substrate-binding and optimal hydride transfer. Moreover, Asn98 was proposed to stabilize the active conformation of catalytic residue Lys176 through a hydrogen bond. Similarly, ManDH2 has a set of conserved corresponding residues, Lys187, Asn105 and Glu273, at equivalent positions (Fig. 4C) in the complex structure with NADH. These ManDH2 residues are located adjacent to each other, suggesting ManDH2 has the same hydrogen bonding networks as EcKPR. In the apo ManDH2 structure, Lys187, Asn105 and Glu273 are far apart from each other, indicating these residues shift closer to each other through the hinge domain closure during NADH binding. Thus, the hinge domain closure seems to be important for the correct placement of these residues for substrate binding and the catalytic reaction. To confirm the function of Lys187, we constructed the K187A mutant, and measured its activity. As a result, the K187A mutant was found to have completely lost its activity, suggesting Lys187 acts as the general acid, as observed in Lys176 of EcKPR. Residues recognizing the C2 hydroxyl and carboxylate groups of a 2-hydroxyacid substrate in the EcKPR structure are also conserved and can be closely superimposed on those in the ManDH2 structure. These observations suggest ManDH2 adopts the same reaction mechanism as KPRs.

On the other hand, the mode of recognition of the side-chain of a substrate appears to be distinct between ManDH2 and EcKPR, in agreement with their different substrate specificities (Fig. 4C). In EcKPR, the C3 dimethyl group makes hydrophobic contacts with Thr119, Val179, Ile183, Val234 and Thr238, and C4 hydroxyl group forms hydrogen bonds with Asn194 and Asn241 [21]. These residues are not conserved in ManDH2. In the ManDH2 structure, hydrophobic residues including Met128, Val190, Met194, Met205, Cys248 and Ile254 define the hydrophobic pocket. This hydrophobic pocket seems to accommodate the hydrophobic moiety of a 2-ketoacid with a hydrophobic side-chain. This structural observation is consistent with the substrate preference that ManDH2 exhibits high activity toward 2-ketoisovalerate, benzoylformate and 2-ketoisocaproate [18]. In addition, ManDH2 lacks hydrophilic residues, and thereby excludes hydrophilic side-chain substrates such as 2-ketopantoate, which is a substrate for KPRs. In contrast, EcKPR prefers hydrophilic 2-ketopantoate, and has no activity toward hydrophobic benzoylformate and 2-ketoisocaproate [41], probably because of the presence of hydrophilic residues including Asn194 and Asn241 in the substrate binding pocket. This amino acid diversity could explain the different substrate specificities of ManDH2 and EcKPR. Thus, our work provides an insight into the substrate recognition mechanisms of the new family of D-2-hydroxyacid dehydrogenases acting on C3-branched substrate. In addition, these findings may enable alteration of substrate specificity through rational design for stereospecificsynthesis of various useful C3-branched D-hydroxy acids. However, it is difficult to identify the amino acid residues directly responsible for substrate binding and to elucidate the substrate recognition mechanism in detail. The structural comparison between ManDH2 and EcKPR revealed the structural variation of the proposed substrate binding loop located between α10 and α11 of ManDH2 (Fig. 4D). This loop, which contains Cys248 and Ile254, seems to be located away from the substrate binding pocket, probably because of the absence of substrate. The substrate binding might cause a conformational change of this loop. Determination of the complex structure of ManDH2 with substrates and elucidation of the substrate binding mechanism are our future challenges.

Acknowledgments

This work was performed with the approval of the Photon Factory Program Advisory Committee (Proposal No. 2010G037). This work was partially supported by a Grant-in-Aid (No. 23580120 to H.T.) from the Ministry of Education, Culture, Sports, Science, and Technology of Japan (MEXT).

Appendix A. Supplementary data

Supplementary data associated with this article can be found, in the online version, at http://dx.doi.org/10.1016/j.bbrc.2013.08.019.

References

[1] K.L. Tobey, G.A. Grant, The nucleotide sequence of the serA gene of *Escherichia coli* and the amino acid sequence of the encoded protein, D-3-phosphoglycerate dehydrogenase, J. Biol. Chem. 261 (1986) 12179–12183.
[2] H. Taguchi, T. Ohta, D-Lactate dehydrogenase is a member of the D-isomer-specific 2-hydroxyacid dehydrogenase family, J. Biol. Chem. 266 (1991) 12588–12594.
[3] N. Bernard, T. Ferain, D. Garmyn, P. Hols, J. Delcour, Cloning of the D-lactate dehydrogenase gene from *Lactobacillus delbrueckii* subsp. *bulgaricus* by complementation in *Escherichia coli*, FEBS Lett. 290 (1991) 61–64.
[4] S. Kochhar, P.E. Hunziker, P. Leong-Morgenthaler, H. Hottinger, Primary structure, physicochemical properties, and chemical modification of NAD^+-dependent D-lactate dehydrogenase, J. Biol. Chem. 267 (1992) 8499–8513.
[5] H.P. Lerch, H. Blöcker, H. Kallwass, J. Hoppe, H. Tsai, J. Collins, Cloning, sequencing and expression in *Escherichia coli* of the D-2-hydroxyisocaproate dehydrogenase gene of *Lactobacillus casei*, Gene 78 (1989) 47–57.
[6] J.D. Goldberg, T. Yoshida, P. Brick, Crystal structure of a NAD-dependent D-glycerate dehydrogenase at 2.4 Å resolution, J. Mol. Biol. 236 (1994) 1123–1140.
[7] G.A. Grant, A new family of 2-hydroxyacid dehydrogenases, Biochem. Biophys. Res. Commun. 165 (1989) 1371–1374.
[8] V.O. Popov, V.S. Lamzin, NAD^+-dependent formate dehydrogenase, Biochem. J. 301 (1994) 625–643.

[9] P.J. Baker, Y. Sawa, H. Shibata, S.E. Sedelnikova, D.W. Rice, Analysis of the structure and substrate binding of *Phormidium lapideum* alanine dehydrogenase, Nat. Struct. Biol. 5 (1998) 561–567.
[10] C. Tokuda, Y. Ishikura, M. Shigematsu, H. Mutoh, S. Tsuzuki, Y. Nakahira, Y. Tamura, T. Shinoda, K. Arai, O. Takahashi, H. Taguchi, Conversion of *Lactobacillus pentosus* D-lactate dehydrogenase to a D-hydroxyisocaproate dehydrogenase through a single amino acid replacement, J. Bacteriol. 185 (2003) 5023–5026.
[11] Y. Ishikura, S. Tsuzuki, O. Takahashi, C. Tokuda, R. Nakanishi, T. Shinoda, H. Taguchi, Recognition site for the side chain of 2-ketoacid substrate in D-lactate dehydrogenase, J. Biochem. 138 (2005) 741–749.
[12] T. Shinoda, K. Arai, M. Shigematsu-Iida, Y. Ishikura, S. Tanaka, T. Yamada, M.S. Kimber, E.F. Pai, S. Fushinobu, H. Taguchi, Distinct conformation-mediated functions of an active site loop in the catalytic reactions of NAD-dependent D-lactate dehydrogenase and formate dehydrogenase, J. Biol. Chem. 280 (2005) 17068–17075.
[13] T. Shinoda, K. Arai, H. Taguchi, A highly specific glyoxylate reductase derived from a formate dehydrogenase, Biochem. Biophys. Res. Commun. 355 (2007) 782–787.
[14] V.I. Tishkov, V.O. Popov, Protein engineering of formate dehydrogenase, Biomol. Eng. 23 (2006) 89–110.
[15] J. Domenech, J.A. Ferrer, A new D-2-hydroxyacid dehydrogenase with dual coenzyme-specificity from *Haloferax mediterranei*, sequence analysis and heterologous overexpression, Biochim. Biophys. Acta 1760 (2006) 1667–1674.
[16] N. Bernard, K. Johnsen, J.J. Holbrook, J. Delcour, D175 discriminates between NADH and NADPH in the coenzyme binding site of *Lactobacillus delbrueckii* subsp. *bulgaricus* D-lactate dehydrogenase, Biochem. Biophys. Res. Commun. 208 (1995) 895–900.
[17] Y. Tamura, A. Ohkubo, S. Iwai, Y. Wada, T. Shinoda, K. Arai, S. Mineki, M. Iida, H. Taguchi, Two forms of NAD-dependent D-mandelate dehydrogenase in *Enterococcus faecalis* IAM 10071, Appl. Environ. Microbiol. 68 (2002) 947–951.
[18] Y. Wada, S. Iwai, Y. Tamura, T. Ando, T. Shinoda, K. Arai, H. Taguchi, A new family of D-2-hydroxyacid dehydrogenases that comprises D-mandelate dehydrogenases and 2-ketopantoate reductases, Biosci. Biotechnol. Biochem. 72 (2008) 1087–1094.
[19] D. Matak-Vinković, M. Vinković, S.A. Saldanha, J.L. Ashurst, F. von Delft, T. Inoue, R.N. Miguel, A.G. Smith, T.L. Blundell, C. Abell, Crystal structure of *Escherichia coli* ketopantoate reductase at 1.7 Å resolution and insight into the enzyme mechanism, Biochemistry 40 (2001) 14493–14500.
[20] C.M. Lobley, A. Ciulli, H.M. Whitney, G. Williams, A.G. Smith, C. Abell, T.L. Blundell, The crystal structure of *Escherichia coli* ketopantoate reductase with $NADP^+$ bound, Biochemistry 44 (2005) 8930–8939.
[21] A. Ciulli, D.Y. Chirgadze, A.G. Smith, T.L. Blundell, C. Abell, Crystal structure of *Escherichia coli* ketopantoate reductase in a ternary complex with $NADP^+$ and pantoate bound: substrate recognition, conformational change, and cooperativity, J. Biol. Chem. 282 (2007) 8487–8497.
[22] A.G.W. Leslie, Recent changes to the MOSFLM package for processing film and image plate data, Joint CCP4 + ESF-EAMCB Newsletter on Protein Crystallography, No. 26, 1992.
[23] A. Vagin, A. Teplyakov, Molecular replacement with MOLREP, Acta Crystallogr. D: Biol. Crystallogr. 66 (2010) 22–25.
[24] R.J. Morris, A. Perrakis, V.S. Lamzin, ARP/wARP and automatic interpretation of protein electron density maps, Acta Crystallogr. D: Biol. Crystallogr. 58 (2002) 968–975.
[25] P. Emsley, K. Cowtan, Coot: model-building tools for molecular graphics, Acta Crystallogr. D: Biol. Crystallogr. 60 (2004) 2126–2132.
[26] G.N. Murshudov, A.A. Vagin, E.J. Dodson, Refinement of macromolecular structures by the maximum-likelihood method, Acta Crystallogr. D: Biol. Crystallogr. 53 (1997) 240–255.
[27] W.L. DeLano, The PyMOL Molecular Graphics System, DeLano Scientific LLC, Palo Alto, CA, 2002.
[28] L. Holm, C. Sander, Dali: a network tool for protein structure comparison, Trends Biochem. Sci. 20 (1995) 478–480.
[29] K.L. Britton, Y. Asano, D.W. Rice, Crystal structure and active site location of *N*-(1-D-carboxylethyl)-L-norvaline dehydrogenase, Nat. Struct. Biol. 5 (1998) 593–601.
[30] F. Colonna-Cesari, D. Perahia, M. Karplus, H. Eklund, C.I. Brädén, O. Tapia, Interdomain motion in liver alcohol dehydrogenase, J. Biol. Chem. 261 (1986) 15273–15280.
[31] V.S. Lamzin, Z. Dauter, V.O. Popov, E.H. Harutyunyan, K.S. Wilson, High resolution structures of holo and apo formate dehydrogenase, J. Mol. Biol. 236 (1994) 759–785.
[32] T.J. Stillman, A.M. Migueis, X.G. Wang, P.J. Baker, K.L. Britton, P.C. Engel, D.W. Rice, Insights into the mechanism of domain closure and substrate specificity of glutamate dehydrogenase from *Clostridium symbiosum*, J. Mol. Biol. 285 (1999) 875–885.
[33] G. Scapin, M. Cirilli, S.G. Reddy, Y. Gao, J.C. Vederas, J.S. Blanchard, Substrate and inhibitor binding sites in *Corynebacterium glutamicum* diaminopimelate dehydrogenase, Biochemistry 37 (1998) 3278–3285.
[34] H. Eklund, J.P. Samama, T.A. Jones, Crystallographic investigations of nicotinamide adenine dinucleotide binding to horse liver alcohol dehydrogenase, Biochemistry 23 (1984) 5982–5996.
[35] Z. Chen, W.R. Lee, S.H. Chang, Role of aspartic acid 38 in the cofactor specificity of *Drosophila* alcohol dehydrogenase, Eur. J. Biochem. 202 (1991) 263–267.
[36] N. Holmberg, U. Ryde, L. Bülow, Redesign of the coenzyme specificity in L-lactate dehydrogenase from *Bacillus stearothermophilus* using site-directed mutagenesis and media engineering, Protein Eng. 12 (1999) 851–856.
[37] C. Ma, L. Zhang, J. Dai, Z. Xiu, Relaxing the coenzyme specificity of 1,3-propanediol oxidoreductase from *Klebsiella pneumoniae* by rational design, J. Biotechnol. 146 (2010) 173–178.
[38] E. Ehsani, M.R. Fernández, J.A. Biosca, S. Dequin, Reversal of coenzyme specificity of 2,3-butanediol dehydrogenase from *Saccharomyces cerevisae* and in vivo functional analysis, Biotechnol. Bioeng. 104 (2009) 381–389.
[39] P.J. Baker, K.L. Britton, D.W. Rice, A. Rob, T.J. Stillman, Structural consequences of sequence patterns in the fingerprint region of the nucleotide binding fold: implications for nucleotide specificity, J. Mol. Biol. 228 (1992) 662–671.
[40] C.R. Faehnle, J. Le Coq, X. Liu, R.E. Viola, Examination of key intermediates in the catalytic cycle of aspartate-β-semialdehyde dehydrogenase from a gram-positive infectious bacteria, J. Biol. Chem. 281 (2006) 31031–31040.
[41] R. Zheng, J.S. Blanchard, Substrate specificity and kinetic isotope effect analysis of the *Escherichia coli* ketopantoate reductase, Biochemistry 42 (2003) 11289–11296.